How to avoid distortions of trap probing due to instrumental recovery time during Deep-Level Transient Spectroscopy measurements

Preprint · August 2023

DOI: 10.13140/RG.2.2.24131.78884

CITATIONS
0

READS
27

1 author:

Teimuraz Mchedlidze
Technische Universität Bergakademie Freiberg
140 PUBLICATIONS **996** CITATIONS

SEE PROFILE

How to avoid distortions of trap probing due to instrumental recovery time during Deep-Level Transient Spectroscopy measurements

Teimuraz Mchedlidze

Institute for Applied Physics, Technical University Bergakademie Freiberg, Freiberg 09599, Germany

Abstract

Utilization of a multi-functional Impedance analyzer and dual-phase digital lock-in amplifier (MFIA) from Zurich Instruments for deep-level transient spectroscopy (DLTS) measurements, allows substantial improvements in the measurement parameters (i.e., a decrease of instrumental recovery time and an increase of transient sampling rate). Based on the results of measurements using such systems, DLTS "signatures" of traps with specific properties (i.e., strong temperature-dependent carrier cross-section, extended structure, etc.) will require reconsideration and correction.

Introduction

Deep-level transient spectroscopy (DLTS) is a well-established electrical measurement method that allows the identification and characterization of carrier traps existing in semiconductor materials and devices [1], [2], [3]. The DLTS, invented by Lang in 1974 [4], successfully supplemented and simplified junction spectroscopy methods allowing the representation of the existing defect states as peaks in the temperature spectrum. The method makes it possible to detect traps with a concentration five orders of magnitude lower than the dopant concentration. Ease of interpretation, high sensitivity, the applicability of standard pn- and Schottky junctions for the measurements, and a relatively simple instrumental system soon made DLTS popular and widely used [3]. Usually, DLTS allows trap-associated defect identification based on their "signature" obtained from the Arrhenius plot [1], [2] and determining trap concentrations based on the amplitude of the related capacitance transients. Further analyses can help in the estimation of the role of the traps in the processes of carrier trapping, recombination, and generation [1]. However, the initial hopes to build a database of "signatures" of defects by characteristic DLTS spectra were not yet fully implemented due to the several drawbacks of the technique.

One of the drawbacks of the DLTS method is its poor resolution for defects with close carrier-emission parameters. This seriously complicates the separation and identification of defects. One of the reasons for the poor resolution was the instrumental broadening due to the analog processing used in Lang's method. After the development of fast and direct transient registration and averaging

methods, significant efforts were devoted to finding effective numerical correlation functions to increase the resolution of the method [5], [6]. Finally, a technique based on the inverse Laplace transform of the repeatedly averaged transient measured at fixed and highly-stable temperature (LDLTS) [7] allowed improvements in the trap resolution by about one order of magnitude in the case of low electric noise and very stable temperature of LDLTS measurements [8]. Usually, standard DLTS measurements precede those of LDLTS to detect (identify) the defect(s) and determine the proper settings for temperature.

Another common technical drawback of the standard DLTS system is the relatively long instrumental recovery time and low time resolution. For a long time, capacitance meters based on capacitance-bridge were utilized in DLTS systems. Standard response times of such systems are in the range from 1 to 10 ms [2] and even after modification response times less than 100 µs rarely can be achieved. Besides that, trap-filling pulses cause overloads of capacitance meters and require delays for the system recovery. These delays can be partially avoided by installing special circuitry [9]. In any case, using capacitance bridge devices it is hardly possible to reach system response times in the < 100 µs range [10]. It should be emphasized that the capacitive bridge itself limits the response speed of the system, so subsequent measurement of the transient with high resolution does not improve the overall result. This drawback limits the possibility and accuracy of detecting transients immediately after the end of the filling pulse. As we will show in this report, this drawback has a critical impact on the detection of defects with special properties.

Significant progress in fast signal processing was achieved in the last years. This allowed a further decrease in electric noise and an increase in signal detection rate (sampling rate). For DLTS applications especially promising are detection systems based on lock-in amplifiers [11]. A possibility of application of the MFIA lock-in amplifier for DLTS and LDLTS measurements was already presented [12], [13], [14].

We recently assembled a DLTS system based on an MFIA lock-in amplifier from Zurich Instruments. The prototype of our system was previously described in [14]. Moreover, the group from Oslo University headed by Prof. E. Monakhov kindly provided LabView software for DLTS measurements developed in their laboratory, which largely simplified the start-up of this study. In the kindly provided software, we modified temperature control, signal processing, data averaging/handling, and saving.

To calibrate and check the capabilities of the new system we used a p-type Si sample contaminated with gold. Gold atoms form efficient recombination centers in Si. DLTS measurements of gold-related traps in silicon have a long history and are well documented (see [15] for a short review and recent status). During the measurements of gold-contaminated sample on our MFIA-DLTS system we detected a trap with a very specific DLTS-signal pattern, besides the well-known gold-related Au(0/+) trap. Below we present obtained results and our tentative explanations.

Samples and experimental

For the present study, we used B-doped (N_a=1×10^{15} cm^{-3}) FZ-Si sample contaminated by gold. Gold was introduced from the pre-deposited Au layer during 60 min annealing at 750˚C in the Ar atmosphere. The expected concentration of gold atoms according to the saturation level was 1×10^{13} cm^{-3} [16]. Schottky-contacts were fabricated by resistive evaporation of Al film through a shadow mask onto the polished and etched surface of the sample. Ohmic contacts were made by rubbing an eutectic InGa-alloy onto the backside of the samples.

Our MFIA-DLTS system was similar to those previously described [13], [14]. In the present study, we used a sample holder that was immersed in the dewar with liquid nitrogen. The temperature was controlled using a heater mounted inside the holder which was connected to the Lakeshore 336 temperature controller. It was possible to set and sweep temperatures in the range from 78 to 390 K. At each temperature step, up to 500 digitized transients were recorded and the averaged transient was saved to a file. Temperature variations during a single step were < 0.3 K. Time necessary for the single-step processing depended on the system parameters, but was in the range of several minutes. For the transformation of digitized transients to DLTS spectra we used correlation with sinus as a weighting function [5] with integration for the chosen rate window. The amplitude of the signal was normalized to the value of capacitance at the measurement temperature.

The main advantage of the MFIA-based DLTS system is a significantly shorter response time (≤ 10 µs) combined with a high sampling rate and short delay time after the filling pulse [11]. Therefore, the instrumental recovery time for such system is drastically shortened. Three different regimes (SET1-SET3) were used on the MFIA system to reveal characteristics of the system at various settings and to compare with the results from a standard DLTS system. The settings for the various parameters used for SET1-SET3 are listed in Table 1.

We studied the same sample on a commercially available HERA-DLTS system from PhysTech [10] for a comparison. The capacitance transients were sampled with 512 points for two sampling periods (24.5 ms and 247 ms) using two delay times (816 µm and 3 ms correspondingly). These settings were suggested as a standard for the temperature scan DLTS measurements on HERA system by the producers.

PARAMETER	SET1	SET2	SET3
$\mathbf{t_{delay}}$, ms	2	0.075	0.075
SR, kSa/s	6.6	13.4	53.6
MBW, kHz	6	13	50
$\mathbf{t_W}$, s	1.02	0.2	0.2

Table 1. Experimental parameters used during the measurements on MFIA based DLTS system. In the table: t_{delay} is interval from the end of a filling pulse till the first data readout; SR is an MFIA sampling rate, MBW is an MFIA bandwidth limit (maximal bandwidth), and t_W is a total sampling time for the settings.

The rest of the measurement parameters were similar for both DLTS systems: we applied a reverse voltage of 5 V, and the filling pulse voltage was 0.5 V. Duration of the filling pulse was 1 ms. DLTS spectra were detected in the temperature range of 80÷300 K, with 1 K steps.

Results and discussion

DLTS spectra obtained from the sample under SET1-SET3 settings are presented in Fig.1 (a)-(c). Spectra detected from the HERA system with close rate windows are presented in Fig1 (d). To avoid ambiguity, we used the DLTS spectra generated by the HERA system directly [10], without further recalculation. From Fig.1 we can state that the Au(0/+) peak (located at lower temperatures), attributed to the gold donor in p-Si [15], is well reproduced in all (a)-(d) spectra. Moreover, for the spectra in (a)-(c), the amplitude of the peak is the same and the estimated trap concentration well coincides with that expected (see Table 2). Estimation of the Au(0/+) related trap concentration from the measurements done on the HERA system using built-in algorithm also gave a close value. The Arrhenius plots built for the Au(0/+) trap under different MFIA system settings and for the data obtained from the HERA system were the same and well coincided with the reference data (see Fig. 2 and Table 2). Therefore for the case of Au(0/+) defect the DLTS “signature” of the trap [15] and estimated concentrations [16] well coincided.

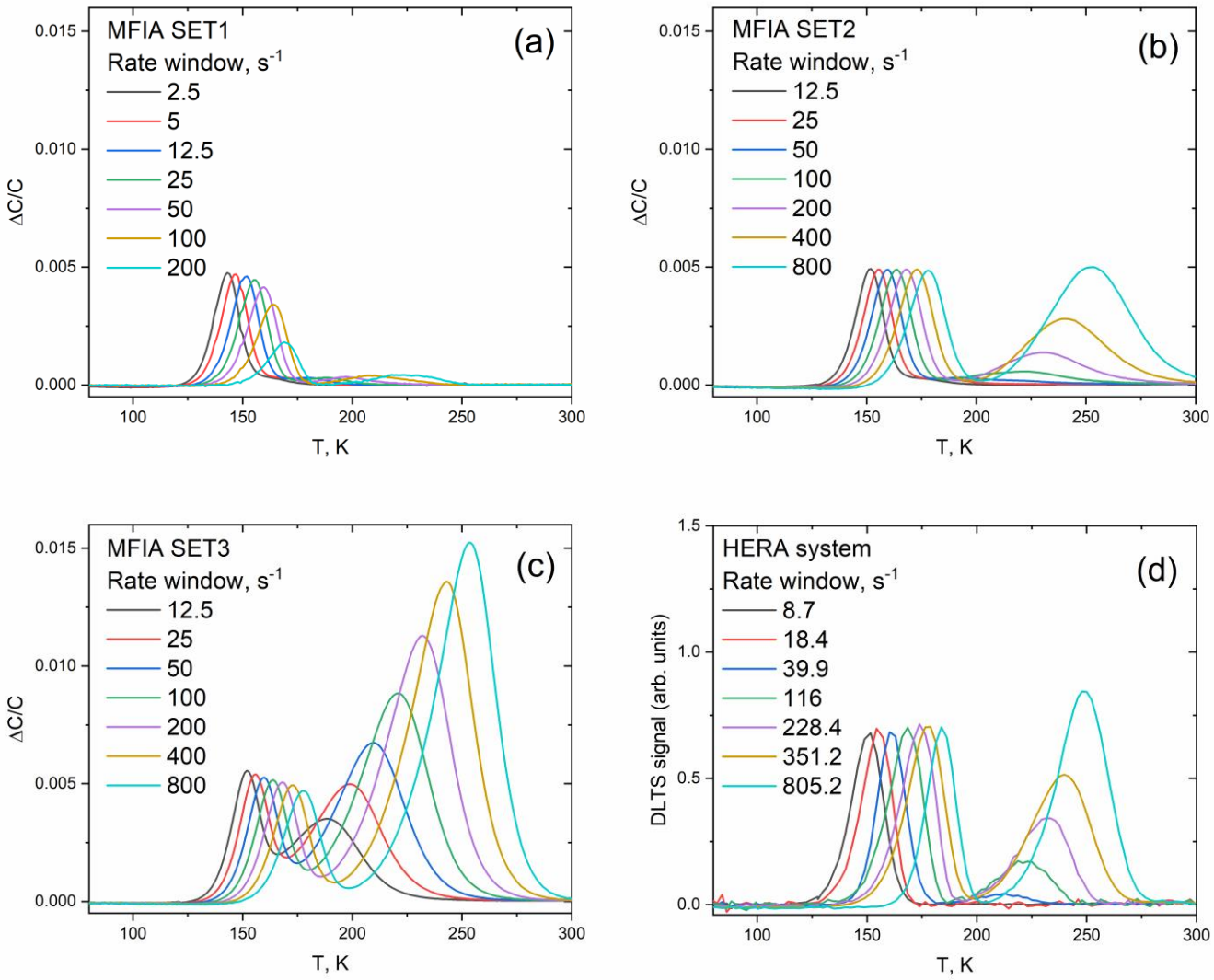

Figure 1. (a)-(c) present DLTS signals detected from the sample using MFIA-based system for various rate windows and the SET1-SET3 settings, see Table 1. (d) presents DLTS spectra extracted from the measurements on HERA system for the same sample.

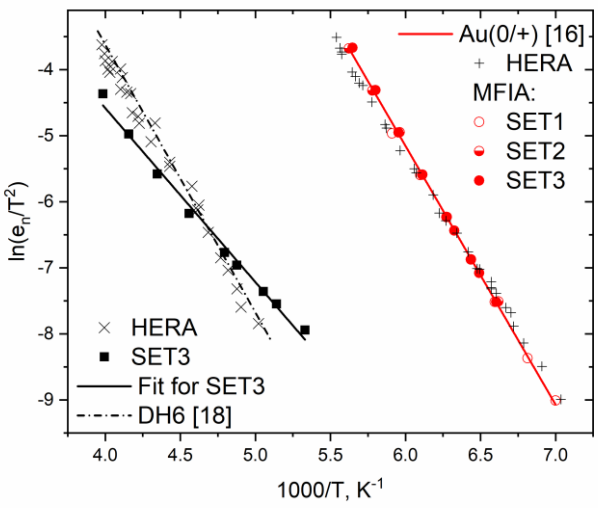

Figure 2. Arrhenius plots (symbols) for the DLTS peaks detected in the sample using HERA and MFIA systems (attributions are indicated in the figure). Lines present data from the references [15], [17] and our fit for the DH6 trap data obtained on MFIA DLTS system.

On the other hand, it is easy to notice substantial differences in the results among the SET1-SET3 settings for the DLTS peak located at higher temperatures in Fig.1 (a)-(c). Based on the Arrhenius plot obtained from the HERA system results, the DLTS signature of the trap well coincides with that of the DH6 hole trap [17], [18] (see also Table 2). The DH6 signature was attributed to dislocation-related traps in silicon in annealed state [17]. The identification of the trap was not the aim of the present study and we do not insist on the identification. However, since the presence of dislocations in the FZ-Si sample cannot be excluded we can suppose that the identification is correct, and, for simplicity, we will label the second DLTS peak as DH6 below. We wanted to understand the reason for the large variations in the DH6 peak positions and intensities between various settings.

TRAP	E_{na}, eV	σ_{na}, cm^{-2}	C_t, cm^{-3}
Au(0/+) MFIA	0.34	6.2×10^{-14}	9.8×10^{12}
Au(0/+) HERA	0.334	7.5×10^{-14}	8×10^{12}
Au(0/+) [15]	0.34	6.2×10^{-14}	(1×10^{13})*
DH6 MFIA	0.23	2×10^{-19}	2.9×10^{13}
DH6 HERA	0.33	3×10^{-16}	1×10^{13}
DH6 [17], [18]	0.35	1.7×10^{-16}	Unknown

Table 2. Detected trap signatures and concentrations of the related defects in the sample. Trap parameters from the references [15], [18] are also presented. For estimation of the DH6 MFIA parameters the results obtained for SET3 settings were used. * - The expected trap concentration from the saturation data [16].

The similarity of Au(0/+) related signals and the diversity of DH6-related signals in DLTS spectra could be clearly depicted if we compare experimentally detected capacitance transients for the SET1-SET3 settings. These transients detected in the temperature range 130-280 K, with the step of 10 K are presented in Fig. 3 (a)-(c). For the transient related to the Au(0/+) trap (temperature range 130-210 K) the curves look very similar. Therefore the delay time, sampling rate, and maximal bandwidth have a small if any influence on the transients, and after the correlation procedure, we obtain the same parameters of the Au(0/+) related DLTS peak. The transients from the DH6 trap drastically differ for the three settings.

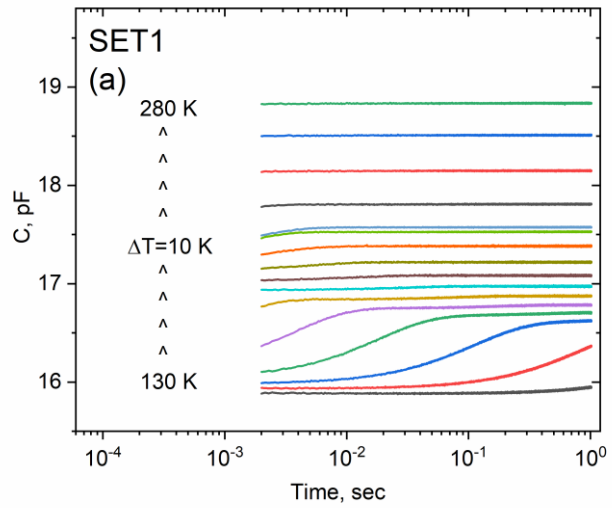

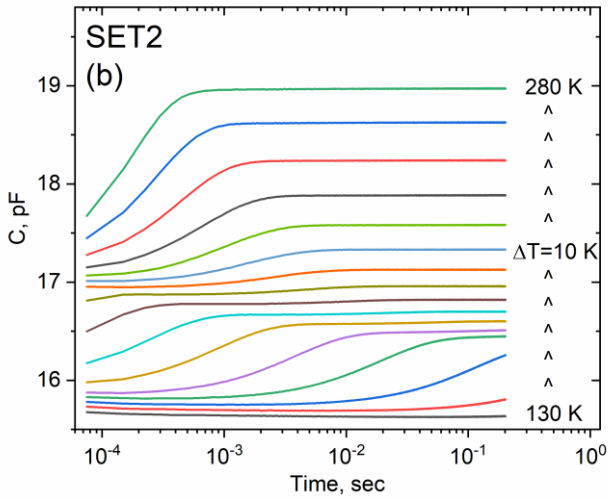

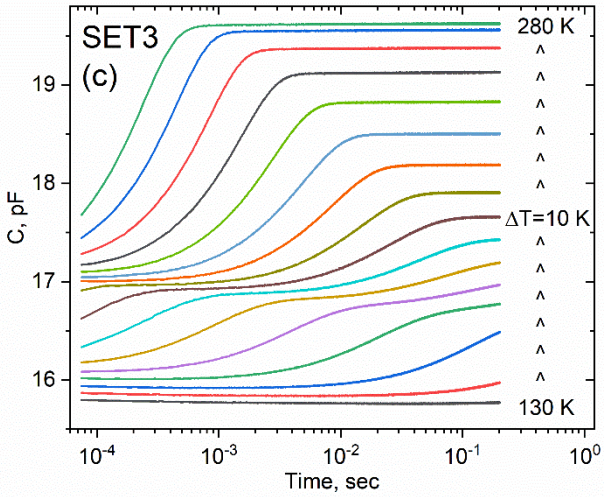

Figure 3. Experimental capacitance transient records detected from the sample at various temperatures (the difference in temperature between the presented curves in the figures is 10K) and for various settings SET1-SET3 on the MFIA system (see Table 1). No additional noise filtering/smoothing was applied.

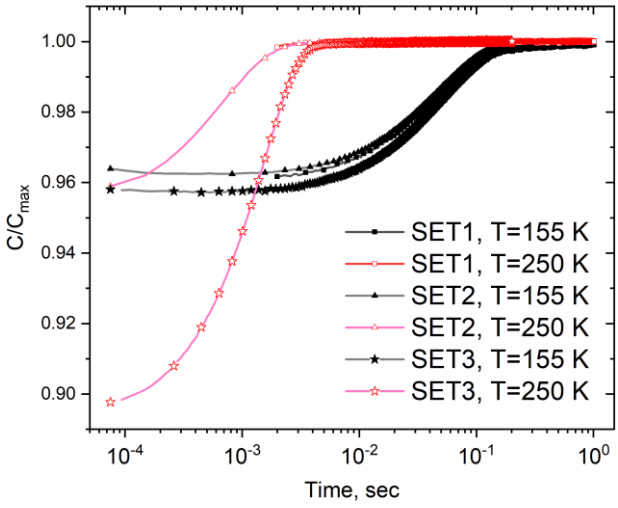

Figure 4. Normalized capacitance transients detected from the sample at 155 K (black color) and 250 K (red color) for SET1-SET3 settings (see Table 1). Note that symbols are shown for every 10th point of the experimental readings. The lines, connecting the readings, are not smoothed.

A few explanatory remarks should be given before further discussion:

- The scale for the (a)-(c) plots in Fig. 3 is the same to simplify comparison. We do not have a certain explanation for the difference in the C_{MAX} values for different settings. However, the measurements were performed after separate mountings of the sample on the holder. That potentially can give a ~1 pF variation for the capacitance detection circuit due to the cable configurations.
- We wanted to keep the delay time as short as possible for the SET2 and SET3 settings. Due to this some residual "tails" from the filling pulse are visible in Fig. 3 (b) for SET2 for times < 0.9 ms at 130-150 K and at 230 K. For SET1 the t_{dalay} = 2 ms was used in an attempt to completely exclude the influence of the filling pulse.
- Properties of the DH6 trap causing observed behavior of the capacitance transients deserve further investigation and that exceeds the topic of the present report. We attribute the observed pattern to the temperature dependent carrier capture cross section for the DH6 defects and to the extended structure of the defects (see [1], [2], and [17] for details).

Let us discuss the obvious difference between the DLTS DH6 defect "signatures" obtained during the performed measurements. The E_{na} and σ_{na} parameters for the DH6 trap obtained from MFIA SET3 and HERA measurements significantly differ (see Fig. 2 and Table 2). The "signatures" for the DH6 trap obtained from the results of measurements in SET1 and SET2 settings are uncertain: on Arrhenius plot the data points cannot be fitted by a single line. That means that for the DH6-like traps, the signatures will be setting-dependent and may be misleading. In our opinion, MFIA SET3 measurement results reflect the properties of the trap closer to reality than those from HERA.

Transients normalized to the C_{MAX} at 155 K and 250 K for SET1-SET3 settings are presented in Fig. 4. From this figure it is clear that, contrary to Au(0/+), for DH6 trap the data for detection times below 2 ms from the filling pulse are crucial. Despite the same t_{delay} for SET2 and SET3, the amplitude of the DH6-related transient for SET2 is much smaller. This should be the effect of SR + MBW settings (see Table 1). Indeed, as seen for the transient at 155 K of SET2, the initial points of the transient curve lean upward. That means that for SET2 settings initial registered points of the transient are affected by the filling pulse tail due to small MBW. Interestingly the apparent settings of the HERA system, with t_{delay}= 816 µm and t_W=24.5 ms, which gives for 512 points SR=21 kSa/s, are intermediate between SET2 and SET3 of MFIA system. Similarly, to the MFIA SET2 results, the DH6 peak cannot be detected for rate windows < 39 s^{-1} on HERA system (see Fig. 1).

We tentatively attribute the observed “peculiar behavior” of the DH6 trap during DLTS measurements to the possible temperature-dependent carrier capture cross-section and/or to the extended structure of the related defects. Indeed, if the cross-section increases with temperature, the amplitude of the related transient will increase as well causing the effect similar to that presented in Fig. 3 (b), (c). On the other side, change of “mobility” of captured carriers along the extended defects due to the applied bias with the temperature may initiate the similar effects. Moreover, both these mechanisms can be involved simultaneously for the case of extended defects.

A temperature-dependent carrier capture cross-section was reported for many defects (see, e.g., [1], [19]). The group of defects with an extended structure is also large (interfaces, precipitates, dislocations, etc.). Our recent study of degraded Si PV cells (not yet published) shows that some degradation-related defects may have properties that place them in one of the above groups, in accordance with the results of [20]. This report indicates that the detection and identification of such defects using standard DLTS Systems can be problematic or misleading and systems with short instrumental recovery should be used.

Summary

The presented results suggest the instrumental recovery time should be possibly minimized during the DLTS measurements. The signatures and detection limits of some defects can be seriously affected by such measurement parameters of DLTS system as delay time before transient sampling, i.e., t_{delay}, sampling rate, and maximum bandwidth of the detecting system. For such defects the related capacitance transient immediately after the filling pulse is of critical importance. Defects with the strong temperature dependence of the carrier capture cross-section and defects with an extended structure represent the groups for which the considered effect can suppress the sensitivity and affect the "signature" of the defect during the DLTS study. For such defects, it is essential to use short t_{delay}, and very high MBW and SR parameters, which are usually not available for standard DLTS systems based on capacitance bridge.

Acknowledgments

We highly appreciate the help and support from the group of Prof. Eduard Monakhov (University of Oslo, Norway). Thanks are due to Katrin Gwozdz (Wroclaw University of Technology, Wroclaw, Poland) for supplying gold-contaminated silicon samples.

References:

[1] P. Blood and J. Orton, "Deep Level Transient Spectroscopy of Majority Carrier Traps," in The Electrical Characterization of Semiconductors: Majority Carriers and Electron States, vol. 14, N. March, Ed., San Diego, CA: Academic Press Inc, **1992**, pp. 399-465.

[2] D. K. Schroder, "Defects," in Semiconductor Material and Device Characterization, T. edition, Ed., Hoboken, New Jersey: A John Wiley & Sons, Inc., **2006**, pp. 270-285.

[3] A. R. Peaker, V. P. Markevich and J. Coutinho, "Tutorial: Junction spectroscopy techniques and deep-level defects in semiconductors," Journal of Applied Physics, **2018**, *123*, 161559. DOI: 10.1063/1.5011327

[4] D. V. Lang, "Deep-level Transient spectroscopy: a new method to characterize traps in semiconductors," Journal Applied Physics, **1974**, *45*, 3023. DOI: 10.1063/1.1663719

[5] A. A. Istratov, "The resolution limit of traditional correlation functions for deep level transient spectroscopy," Review of Scientific Instruments, **1997**, *68*, 3861. DOI: 10.1063/1.1148038

[6] A. Istratov and O. Vyvenko, "Exponential analysis in physical phenomena," Review of Scientific Instruments, **1999**, *70*, 1233. DOI: 10.1063/1.1149581

[7] L. Dobaczewski, A. R. Peaker and K. Bonde Nielsen, "Laplace-transform deep-level spectroscopy: The technique and its applications to the study of point defects in semiconductors," Journal Applied Physics, **2004**, *96*, 4689. DOI: 10.1063/1.1794897

[8] V. Peaker, V. Markevich, I. Hawkins, B. Hamilton, K. Bonde Nielsen and K. Gościński, "Laplace deep level transient spectroscopy: Embodiment and evolution," Physica B: Condensed Matter, **2012**, *407*, 3026. DOI: 10.1016/j.physb.2011.08.107

[9] T. I. Chappell and C. M. Ransom, "Modifications to the Boonton 72BD capacitance meter for deep-level transient spectroscopy applications," Review of Scientific Instruments, **1984**, *55*, 200. DOI: 10.1063/1.1137716

[10] PhysTech, "FT 1030 Deep-Level Transient Spectroscopy System," PhysTech, **2008**. [Online]. Available: http://www.phystech.de/products/dlts/dlts.htm. [Accessed 07 08 2023].

[11] Z. Instruments, "Principles of lock-in detection and the state of the art," **2016**. [Online]. Available: https://www.zhinst.com/applications/principles-of-lock-in-detection. [Accessed 07 08 2023].

[12] Z. Instruments, "Laplace Deep Level Transient Spectroscopy using the MFIA," **2017**. [Online]. Available: https://www.zhinst.com/sites/default/files/zi_mfia_appnote_dlts.pdf. [Accessed 07 08 2023].

[13] G. Nelson, G. Ouin, S. Polly, K. Wynne, A. Haberl, W. Lanford, R. Lowell and S. Hubbard, "In Situ Deep-level Transient Spectroscopy and Dark Current Measurements of Proton-Irradiated InGaAs Photodiodes," IEEE Transactions on Nuclear Science, **2020**, *67*, 2051. DOI: 10.1109/TNS.2020.3011729

[14] C. Matre, Deep-level transient spectroscopy system with a response time in the microsecond time frame, Oslo: University of Oslo, **2019**.

[15] K. Gwozdz, V. Kolkovsky, V. Kolkovsky and J. Weber, "Revised identification of the G-levels in gold doped Si by Laplace deep level transient spectroscopy," Journal Applied Physics, **2018**, *124*, 015701. DOI: 10.1063/1.5036807

[16] N. Stolwijk, B. Schuster, J. Hölzl, H. Mehrer and W. Frank, "Diffusion and solubility of gold in silicon," Physica B, **1983**, *116*, 335. DOI: 10.1016/0378-4363(83)90271-1

[17] V. Kveder, Y. Osipyan, W. Schröter and G. Zoth, "On the energy spectrum of dislocations in Silicon," Physica Status Solidi (a), 1982, 72, 701. DOI: 10.1002/pssa.2210720233

[18] K. Goscinski, "Defect DLTS signal Standards," IFPAN, Warsaw, Poland, **2023**. [Online]. Available: http://www.laplacedlts.eu/defectTV/. [Accessed 17 08 2023].

[19] B.B. Paudyal, K. R. McIntosh, and D. H. Macdonald, “Temperature Dependent Electron and Hole Capture Cross Sections of Iron-Contaminated Boron-Doped Silicon”. In 34th IEEE Photovoltaic Specialists Conference; **2009**; p. 001588. DOI: 10.1109/PVSC.2009.5411380.

[20] Y. Buratti, J. Dick, Q.L. Gia, and Z. Hameiri, “Deep Learning Extraction of the Temperature-Dependent Parameters of Bulk Defects,” ACS Appl. Mater. Interfaces, **2022**, *14*, 48647. DOI: 10.1021/acsami.2c12162